Biophysical Chemistry 142 (2009) 34–39

Contents lists available at ScienceDirect

Biophysical Chemistry

journal homepage: http://www.elsevier.com/locate/biophyschem

Oligomerisation and thermal stability of polyvalent integrin α5β1 ligands

Michaela Kreiner [a], Olwyn Byron [b], Diana Domingues [a], Christopher F. van der Walle [a,*]

[a] Institute of Pharmacy and Biomedical Sciences, University of Strathclyde, 27 Taylor Street, Glasgow, UK
[b] Division of Infection and Immunity, Institute of Biomedical and Life Sciences, University of Glasgow, G12 8QQ, UK

ARTICLE INFO

Article history:
Received 10 January 2009
Received in revised form 27 February 2009
Accepted 1 March 2009
Available online 11 March 2009

Keywords:
Coiled coil
Fibronectin
Integrin
Analytical ultracentrifugation
Thermal unfolding

ABSTRACT

Synthetic oligomeric integrin α5β1 ligands, specifically immobilised to surfaces, facilitate increased fibroblast cell spreading compared with that associated with the monomer. These ligands consist of a N-terminal fibronectin domain pair, a spacer and a di-, tri- or tetrameric coiled coil. However, it is not yet clear what effect fusion of the fibronectin domains has on the predicted oligomerisation of the coiled coils. Using analytical ultracentrifugation we show that the predicted tetrameric and trimeric coiled coils facilitate a corresponding ligand oligomerisation with half-dissociation at 0.7 and 0.2 μM, respectively. In contrast, the predicted dimeric coiled coil formed both dimers and trimers. Under non-reducing conditions, the unique C-terminal thiol-facilitated inter-oligomer dimerisation of the trimeric species, generating hexameric ligands. Disulphide bonding also increased helical stability during thermal unfolding. The work allows the cellular response to these clustered integrin α5β1 ligands to be more accurately interpreted, and has wider implications with respect to the utility of coiled coils as tools to facilitate protein oligomerisation.

1. Introduction

Coiled coils provide versatile fusion partners for oligomerisation since they are small domains with predictable quaternary structure [1]. They are supercoiled bundles of two to five α-helices with a packing geometry of core residues, termed knobs-into-holes, resulting in a strong sequence periodicity called the 'heptad repeat' [2]. A coiled-coil protein that has been used frequently and successfully in such fusions is the GCN4 leucine zipper [3]. The oligomeric form of this coiled coil can be altered between di-, tri- or tetramer by mutating the branched, hydrophobic residues and positions *a* and *d* of the heptad repeat [4]. While coiled coil motifs have been used successfully to oligomerise proteins (e.g. [5]), data describing effects of the fused protein on the association state and dissociation constant of the coiled coil peptide are sparse.

For cell adhesion mediated by integrin binding to extracellular matrix proteins, clustering of the integrin receptors is a key step bringing about 'adhesion reinforcement' [6,7]. Initially, these studies utilised the RGD motif, in a clustered display, to promote adhesion primarily through αvβ3 integrin. However, to promote cell adhesion through α5β1 integrin, the minimal binding domain includes the synergy site (PHSRN) on the 9th type III FN domain in addition to the RGD on the 10th type III FN domain [8]. Thus, the generation of equivalent clustered α5β1 integrin ligand displays necessitates the engineering of protein chimeras. Previously, very large chimeras have been studied employing four type III FN domains (FIII7-10), a large spacer of six titin repeats (58 kDa) and coiled coil [9]. In contrast, we have designed much smaller and more flexible, clustered α5β1 integrin ligands consisting of: the 9th–10th type III FN domain pair (FIII9'-10, a L1408P mutant with increased conformational stability and cell adhesion activity [10]), a spacer derived from the IgG-hinge (previously shown to be sufficient to prevent steric clashes between bound integrins [11]) and five heptad repeats based on the GCN4 leucine zipper (with isoleucine and leucine variously placed in positions *a* and *d* to promote di-, tri- and tetramerisation [4]). For controlled immobilisation of these chimeras to a substrate or surface a unique C-terminal cysteine was introduced to facilitate either selective biotinylation via a thioether bond, followed by binding to avidin-coated surfaces, or direct covalent binding via the free thiol to gold surfaces [12].

Here we present data describing how the fusion of a 183 residue, β-sandwich domain pair (FIII9'-10) modulates the oligomerisation state of leucine zippers designed to form dimers, trimers or tetramers. Analytical ultracentrifugation (AUC) and thermal denaturation were used to measure the oligomerisation state of the chimeras and probe their thermal stability.

2. Materials and methods

2.1. Materials

Three chimeras were made: FIII9'-10-dimer, FIII9'-10-trimer and FIII9'-10-tetramer, whose construction and expression have been described previously [12]. General chemical reagents were sourced from Sigma-Aldrich, UK, at analytical standard.

Abbreviations: DTT, dithiothreitol; GdnHCl, guanidine hydrochloride; $s_{20,b}$, experimental sedimentation coefficient for the protein(s) at 293 K in buffer; $s^0_{20,w}$, experimental sedimentation coefficient corrected to standard conditions and extrapolated to infinite dilution; SE, sedimentation equilibrium; SV, sedimentation velocity.

* Corresponding author. Tel.: +44 141 548 5755; fax: +44 141 552 2562.
E-mail address: chris.walle@strath.ac.uk (C.F. van der Walle).

0301-4622/$ – see front matter © 2009 Elsevier B.V. All rights reserved.
doi:10.1016/j.bpc.2009.03.001

2.2. Analytical ultracentrifugation (AUC)

Prior to AUC analysis, the proteins were extensively dialysed against NaCl phosphate buffer (10 mM NaH_2PO_4, 500 mM NaCl, pH 7.8) either in the presence or absence of 1 mM DTT. To ensure complete reduction of the proteins in experiments with DTT, proteins were incubated in 50 mM DTT for 1 h prior to dialysis against NaCl phosphate buffer with 1 mM DTT. AUC studies were performed using an Optima XL-I analytical ultracentrifuge (Beckman Coulter, Palo Alto, CA, USA) and an An-60 Ti rotor.

Sedimentation velocity (SV) experiments were conducted at a temperature of 293 K and rotor speed of 49 k rpm. 360 µl volumes of protein (ranging from 0.05–5.0 mg/ml) and reference solvent (dialysate) were loaded into 12 mm charcoal-filled epon double sector centerpieces. Concentration distributions were recorded every minute over a period of 6 h using interference optics. Radial- and time-independent noise were then subtracted from the resultant data using the program SEDFIT [13] which was then used to model the sedimentation velocity profiles with finite element solutions of the Lamm equation for a large number of discrete, non-interacting species resulting in a continuous size distribution ($c(s)$ versus s). Initial fits were conducted over the range of 0.1–20 S to cover all plausible species. High resolution (resolution = 100) fits were then performed within a narrower range (1–10 S).

Sedimentation equilibrium (SE) data for reduced proteins (1 mM DTT) were obtained at a temperature of 293 K and three rotor speeds (15, 25 and 35 k rpm). 80 µl volumes of protein (ranging from 0.1–1.0 mg/ml) and reference solvent (dialysate) were loaded into 12 mm charcoal-filled epon double sector centerpieces. Concentration distributions were recorded every 3 h using interference optics until equilibrium was satisfactorily attained. Ascertainment of equilibrium was monitored using the program WINMATCH (written by Jeffrey Lary, University of Connecticut, Storrs, CT, USA). SE data were analyzed with SEDPHAT [14]. FIII9'-10-trimer and FIII9'-10-tetramer data were fitted with monomer-trimer or monomer-n-mer ($n = 4$) self-association models, respectively. Global fits were performed for two concentrations (3.3 and 33 µM) and three speeds.

The partial specific volume ($\bar{\nu}$) of the proteins was estimated from their known amino acid sequences. This gave $\bar{\nu} = 0.728$ ml/g for all the proteins. The buffer density (1.02012 g/ml in the presence of DTT; 1.02011 g/ml without DTT) and buffer viscosity (0.010534 P in the presence of 1 mM DTT; 0.010531 P without DTT) were calculated using the freeware program SEDNTERP [15]. These values were used to correct the experimentally determined sedimentation coefficients to standard conditions (i.e. a solvent of water at 293 K).

2.3. Hydrodynamic modeling

A bead model of the monomeric unit of the chimera was constructed based on the amino acid sequence of FIII9'-10-dimer (Fig. 1). Homology models of FIII9'-10 and the 5 coiled coil heptad repeats, based on templates of the wild-type 9th–10th type III FN domain pair (PDB accession code 1fnf) and the GCN4 leucine zipper (PDB accession code 2zta) respectively were predicted using SWISS-MODEL [16]. Beads representing the remaining three N-terminal residues of the coiled coil (RIK), the IgG-derived spacer and the 14-residue N-terminal polyhistidine tag were 'manually' created and positioned using the program MacBeads (written by Dr Dan Thomas (then at the National Centre for Macromolecular Hydrodynamics, University of Leicester, UK), downloadable from http://www.nottingham.ac.uk/ncmh/).

Since the orientation of FIII9'-10 to the coiled coil domain is unknown, two structural extremes were modeled and assessed separately: a 'straight' model with an angle of 180° between FIII9'-10 and the coiled coil, and a 'bent' model with an angle of 90° between FIII9'-10 and the coiled coil (Fig. 2). The IgG-derived spacer between FIII9'-10 and the coiled coil was modeled as a rod with the center of rotation arbitrarily chosen in the middle of the spacer; this was considered reasonable since the IgG hinge is predicted to be highly flexible [17].

A

MRGSHHHHHHGMASGLDSPTGIDFSDITANSFTVHWIAPRATITGYRIRHHPEHFSG
RPREDRVPHSRNSITLTNLTPGTEYVVSIVALNGREESPPLIGQQSTVSDVPRDLEV
VAATPTSLLISWDAPAVTVRYYRITYGETGGNSPVQEFTVPGSKSTATISGLKPGVD
YTITVYAVTGRGDSPASSKPISINYRTSKL<u>EPKSSDTPPGSPRSPEPKSSDTPPGSP
RSG</u>*RIKQLEDKIEELLSKIYHLENEIARLKKLIGELEDKIENL***GC**

B

construct	coiled coil
FIII9'-10 dimer	*RIKQLEDKIEELLSKIYHLENEIARLKKLIGELEDKIENL*
FIII9'-10 trimer	*RIKQIEDKIEEILSKIYHIENEIARIKKLIGEIEDKIENI*
FIII9'-10 tetramer	*RLKQIEDKLEEILSKLYHIENELARIKKLLGEIEDKLENI*

Fig. 1. Design of FIII9'-10 constructs. Amino acid sequence of FIII9'-10-dimer (A), N-terminal polyhistidine tag and C-terminal glycine-cysteine are shown in bold font; the FIII9'-10 domain pair in normal font; the IgG-derived spacer underlined and the coiled coil italicised. The trimer and tetramer differ in the coiled coil (B); all other amino acids being the same as for the FIII9'-10-dimer.

Anhydrous sedimentation coefficients (s) for all bead models were calculated using the program HYDRO [18]. In order to compare the HYDRO output with the values for s obtained experimentally, a correction was made algebraically for hydration [19] according to the following formula: $s_\delta = s_0 \times (\overline{\nu}/(\overline{\nu} + (\delta \times \nu_S)))^{1/3}$, where s_δ is the hydrated sedimentation coefficient, s_0 is the anhydrous sedimentation coefficient (as computed by HYDRO), $\overline{\nu}$ is the partial specific volume, ν_S is the specific volume of the solvent (which approximates to its reciprocal density) and δ is the level of hydrodynamic hydration. A hydration level of 0.4 g H_2O/g protein was assumed.

2.4. Circular dichroism (CD)

CD measurements were carried out on a Chirascan spectropolarimeter (Applied Photophysics, UK). Temperature measurements were recorded at 2 °C increments from 20 to 90 °C. Proteins were diluted to a concentration of 1.0 mg/ml and equilibrated in 6 M guanidine hydrochloride (GdnHCl), 10 mM NaH_2PO_4, 300 mM NaCl, pH 7.0. Quartz cells with a path length of 0.2 mm were used (Hellma, UK) and background CD readings for the 6 M GdnHCl buffer above acquired. Data for the thermal melts were collected at 222 nm using an equilibration time of 2.5 min at each temperature step and a data averaging time of 1 min. Data for the reduced proteins were measured after at least a 1 h incubation of the protein in 1 mM DTT in the 6 M GdnHCl buffer above. The melting temperature (T_m) of the proteins obtained by CD was taken from the inflection point of a plot of the fraction unfolded at 222 nm (corresponding to α-helix) versus temperature.

3. Results and discussion

3.1. Variables affecting the oligomerisation state of the ligands

To elucidate the self-association behavior of the FIII9'-10-dimer, FIII9'-10-trimer and FIII9'-10-tetramer under non-reducing conditions, SV experiments were performed for each over a series of concentrations. The corresponding size distribution profiles are shown in Fig. 3. The FIII9'-10-dimer yielded a complex profile, with three main species with sedimentation coefficients of $s_{20,b} = 2.7$, 3.3 and 4.9 S. The FIII9'-10-trimer showed a major species with $s_{20,b} = 4.9$ S and a minor species with $s_{20,b} = 3.3$ S. The FIII9'-10-tetramer resulted in one major peak with $s_{20,b} = 3.9$ S. Minor peaks were also observed at higher sedimentation coefficients; around $s_{20,b} = 5.5$ S for the FIII9'-10-tetramer and >6 S for the FIII9'-10-dimer and FIII9'-10-trimer. These may represent higher order oligomers (discussed below) but remain a minor component.

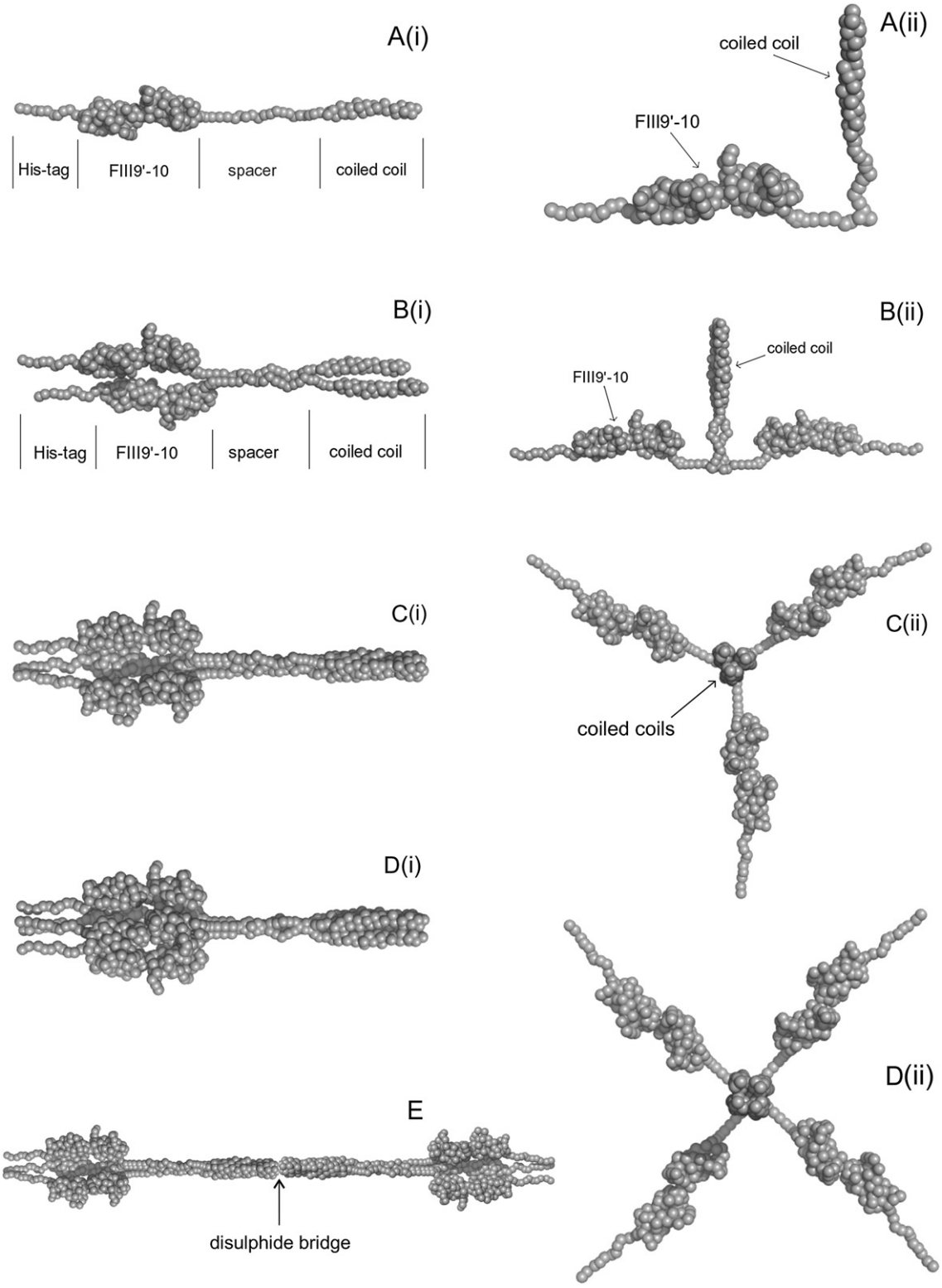

Fig. 2. 'Straight' (i) and 'bent' (ii) bead models for the FIII9'-10-monomer (A), FIII9'-10-dimer (B), FIII9'-10-trimer (C) and FIII9'-10-tetramer (D). The disulphide-linked dimerised trimer was modeled as the straight form only (E). The individual peptide domains (N-terminal polyhistidine tag, FIII9'-10 domain pair, IgG-derived spacer and coiled coil) are indicated by demarcation in A(i) and B(i). The same peptide domains were used to build the bent model, which has a 90° turn at the center of the spacer and the other straight models. Images C(ii) and D(ii) are shown as the elevated plan.

The finding that the main species of FIII9'-10-trimer had a higher sedimentation coefficient ($s_{20,b}=4.9$ S) than FIII9'-10-tetramer ($s_{20,b}=3.9$ S) was initially puzzling. Additionally, species with $s_{20,b}=3.3$ and 4.9 S were observed in the $c(s)$ analysis of SV data for both the FIII9'-10-dimer and trimer. These two initial observations made it necessary to first assign the peaks to plausible species in these systems (i.e. from dimeric to pentameric coiled coil assemblies). The calculated, theoretical sedimentation coefficients, computed for the bead-models, are summarised in Table 1, compared with experimental values corrected to standard conditions and extrapolated to infinite dilution

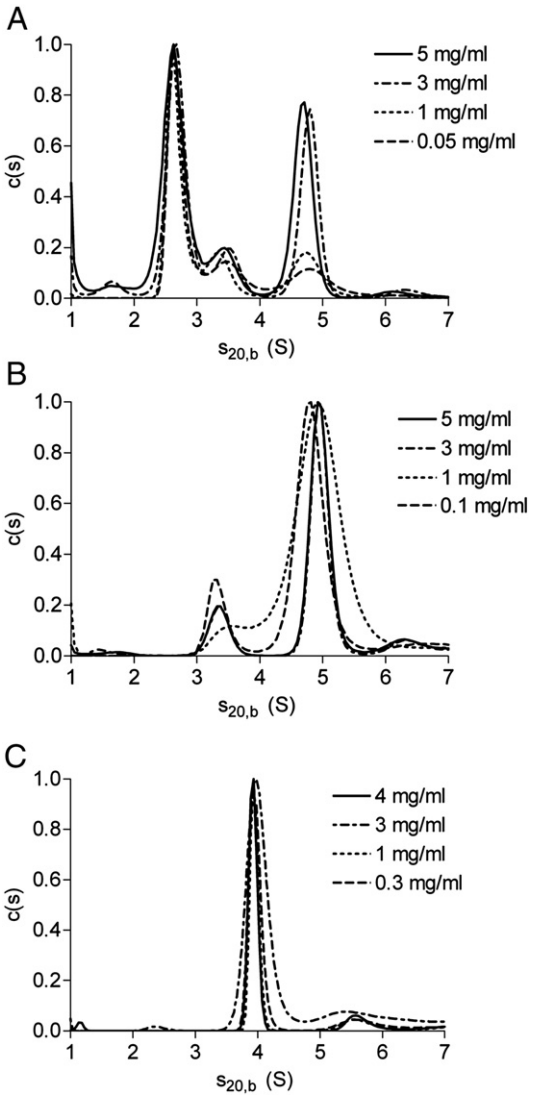

Fig. 3. Size distributions ($c(s)$ versus s) for the FIII9'-10-dimer (A), FIII9'-10-trimer (B), and FIII9'-10-tetramer (C) in 10 mM $NaHPO_4$, 500 mM NaCl, pH 7.8, for protein concentrations as shown. For ease of comparison across the concentration range, the distributions were normalised to the major peak in each case.

($s^0_{20,w}$). The first point of note is that the FIII9'-10 coiled coil constructs appear to be rather anhydrous in solution: agreement with the experimentally determined $s^0_{20,w}$ (1.77, 1.80 S) is not particularly sensitive to the conformation of the monomer (i.e. straight or bent) but occurs only for the anhydrous values. This trend is observed throughout the rest of Table 1, therefore comparison will henceforth be made between the values computed for the *anhydrous* bead models and $s^0_{20,w}$. The predicted hydrophobicity of the constructs can be inferred from fluorescence studies of FIII9'-10, which demonstrate the presence of hydrophobic patches in aqueous solution, and a conditional hydrophobic accessible surface area (CHASA [20]) of 5439 Å^2 [21].

The calculated sedimentation coefficient of the straight FIII9'-10-tetramer model ($s = 4.7$ S) matches the experimental sedimentation coefficients (4.40, 4.28 S) quite well. The main species found by the SV experiments for FIII9'-10-dimer (2.94, 2.86 S) can be reasonably assigned to the "straight" dimeric form with a calculated s of 2.7 S. The sedimentation coefficient of 3.9 S calculated for the 'straight' bead model of the trimeric species, corresponds to the species found experimentally for the FIII9'-10-trimer (3.83, 3.69 S). The major FIII9'-10-trimer species observed (5.44, 5.36 S) match the value calculated for a pentameric species, generated from straight monomers (5.6 S). However, the existence of a pentameric species for FIII9'-10-trimer is inconsistent with the gel filtration experiments previously performed [12]. An alternative hypothesis is that this species is a homodimer of two FIII9'-10-trimeric species, interacting either via the polyhistidine tags [22] or an inter-oligomer disulphide bond via oxidation of two C-terminal cysteines. Interaction between FIII9'-10 domain pairs and/or the IgG-derived spacer is highly unlikely since such interaction would have been previously observed during differential scanning calorimetry and gel filtration experiments for FIII9'-10 [23] and high resolution structural studies of the immunoglobulin [17]. Since no higher order oligomers were observed for the FIII9'-10-dimer or FIII9'-10-tetramer, interaction via the polyhistidine tag is also unlikely. In contrast, inter-oligomer disulphide bond formation between two FIII9'-10-trimeric species is plausible because, on considering an individual trimeric coiled coil assembly, a free thiol would always be retained following oxidation.

Modelling the sedimentation coefficient for two disulphide-bridged FIII9'-10-trimeric species was problematic since it was necessary to estimate the angle between the two trimers. As a result, a single simple straight, end-to-end model was used (Fig. 2). This yielded a calculated sedimentation coefficient of 5.0 S, not far from the experimental value (5.44 S), especially given the assumptions made about the orientation between the trimers. In order to more convincingly demonstrate that two FIII9'-10-trimeric species could dimerise via inter-oligomer disulphide bridge, SV experiments were performed under reducing conditions. In 1 mM DTT, the FIII9'-10-trimer sediments as one major species ($s^0_{20,w} = 3.69$ S) which agrees well with the calculated sedimentation coefficient of 3.9 S for the trimer (Fig. 4). The main species observed under non-reducing conditions (5.44 S) was almost entirely absent under reducing conditions, confirming that this species is likely to be a hexamer composed of two trimers linked via a disulphide bond.

Similarly, under reducing conditions, the profile for the FIII9'-10-dimer showed a near complete loss of the same hexameric species ($s^0_{20,w} = 5.35$ S), with a concomitant increase in the species matching that of a trimer ($s^0_{20,w} = 3.72$ S). Thus, the FIII9'-10-dimer self-assembles to not only the expected dimer but also a trimeric species, and in non-reducing conditions the trimeric species are subject to

Table 1
Sedimentation coefficients calculated (s) for hydrodynamic models of FIII9'-10 coiled coils.

Model	Conformation	s (S)		$s^0_{20,w}$ (S)
		Anhyd[a]	Hyd[b]	
Monomer	Straight[c]	1.7	1.4	1.77[e], 1.80[f]
	Bent[d]	1.8	1.5	
Dimer	Straight[c]	2.7	2.3	2.94[e], 2.86[g]
	Bent[d]	2.5	2.2	
Trimer	Straight[c]	3.9	3.3	3.85[e], 3.83[f], 3.72[g], 3.69[h]
	Bent[d]	3.1	2.6	
Tetramer	Straight[c]	4.7	4.0	4.40[i], 4.28[j]
	Bent[d]	3.7	3.2	
Pentamer	Straight[c]	5.6	4.8	–
	Bent[d]	4.3	3.7	
Dimerised trimer	Straight[c]	5.0	4.3	5.35[e], 5.44[f]

For comparison, experimentally determined values ($s^0_{20,w}$) are given: an explanation of their assignment to particular n-meric species is given in the text.
The corresponding bead models, except the pentamer, are shown in Fig. 2.
[a] Anhydrous value.
[b] Corrected for hydration (assuming 0.4 g water/g protein), details in Materials and methods.
[c] Linear monomeric unit.
[d] 90° angle between coiled coil and FN module (see Materials and methods).
[e] FIII9'-10-dimer (in the absence of DTT).
[f] FIII9'-10-trimer (in the absence of DTT).
[g] FIII9'-10-dimer (in the presence of DTT).
[h] FIII9'-10-trimer (in the presence of DTT).
[i] FIII9'-10-tetramer (in the absence of DTT).
[j] FIII9'-10-tetramer (in the presence of DTT).

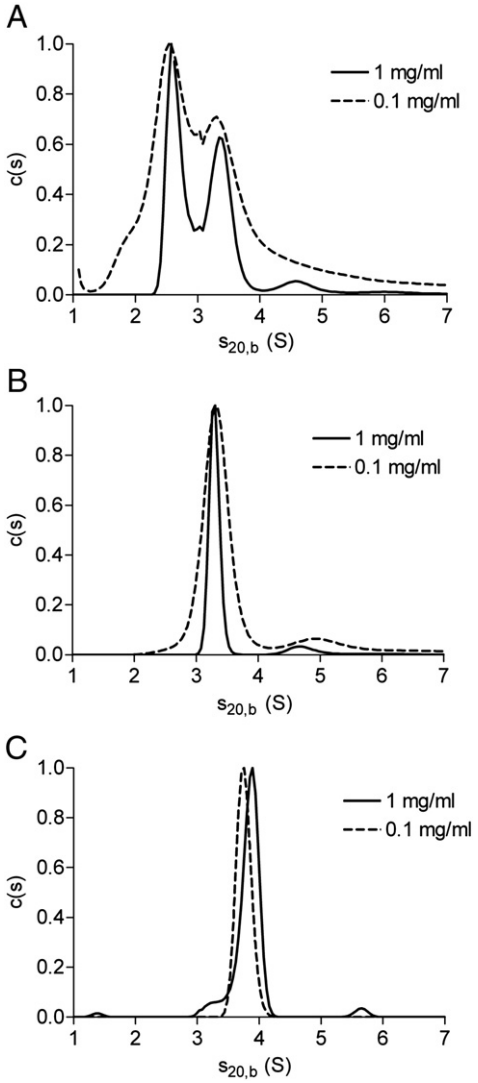

Fig. 4. Size distributions ($c(s)$ versus s) for the FIII9'-10-dimer (A), FIII9'-10-trimer (B), and FIII9'-10-tetramer (C) in 1 mM DTT, 10 mM $NaHPO_4$, 500 mM NaCl, pH 7.8, for protein concentrations as shown. For ease of comparison across the concentration range, the distributions were normalised to the major peak in each case.

inter-oligomer oxidation and formation of hexamers, as for FIII9'-10-trimer. This strongly suggests that the mutated GCN4 coiled domain employed here to facilitate dimerisation [4], when conjugated to FIII9'-10 at least, self-assembles into both dimeric and trimeric oligomers. Thus, the fusion partner of the dimeric coiled coil would appear to influence its oligomerisation state since this transition is not observed for the same series of GCN4-derived peptides alone [4]. An additional explanation is that the pattern of salt-bridges over the heptad repeat at the salt concentrations used here drives oligomerisation of FIII9'-10-dimer towards the trimer. This would be consistent with work showing that the stability of a particular oligomeric state for synthetic coiled coils can be improved by consideration of the ionic interactions [24] and modulated according to the salt concentration of the buffer [25].

3.2. The ligands self-assemble to form stable oligomers

Only the oligomerisation state of the FIII9'-10-dimer was significantly influenced by the protein concentration over the range examined (Fig. 3). At 5 mg/ml protein, approximately half of the protein was in the dimeric state ($s^0_{20,w} = 2.94$ S), with the remainder being largely trimeric ($s^0_{20,w} = 3.85$ S), with a trace amount of the monomer. With decreasing protein concentration, the ratio of dimer to trimer was shifted towards the dimer. The appearance of the monomeric species under non-reducing conditions was only evident for the FIII9'-10-dimer and FIII9'-10-trimer at concentrations ≥3 mg/ml. For the FIII9'-10-tetramer, no monomer was detected at any concentration investigated. The absence of the monomer at lower concentrations was somewhat surprising; although under reducing conditions for the FIII9'-10-dimer at 0.1 mg/ml, a shoulder consistent with monomer was observed in the $c(s)$ profile (Fig. 4).

To properly elucidate the dissociation constant for each of the chimeras, sedimentation equilibrium experiments were performed in presence of 1 mM DTT. Fitting of these SE data yielded a dissociation constant $K_{d(1,3)}$ for FIII9'-10-trimer of 0.03 μM^2 ($K_{d(1,3)}$ = [molar concentration of monomer]^3/[molar concentration of trimer]). The dissociation constant $K_{d(1,4)}$ for the tetramer was estimated as 0.3 μM^3 ($K_{d(1,4)}$ = [molar concentration of monomer]^4/[molar concentration of tetramer]). That is, the FIII9'-10-trimeric species is equimolar with the monomer at 0.2 μM and the FIII9'-10-tetrameric species is equimolar with the monomer at 0.7 μM. Since FIII9'-10-dimer appeared to form both dimers and trimers it was not possible to calculate the K_d using this model. These values agree well with the dissociation behavior inferred from cell adhesion data for a related tetrameric polypeptide assembly (equimolar concentrations at concentrations <0.5 μM) [11]. However, precise K_d values for coiled coils cannot always be easily assigned as we have also noted for the dimer [26]. Initial SE data for GCN4 peptides yielded K_d < 10 μM [27], whereas exceptionally stable GCN4-derived heterodimers with a K_d ~ 0.03 μM have also been characterised [28]. Nevertheless, the oligomeric ligands in this study appear to have stability at least equivalent to the wild type GCN4 peptide. Importantly, the ligands would therefore remain in their oligomeric form over the range of concentrations used in cell adhesion and spreading assays [12].

3.3. The oligomerised ligands are further stabilised by disulphide bonding

The far-UV CD spectrum for the isolated FIII9'-10 domain pair shows no α-helical contribution [23]. Therefore, the appearance of any α-helical bands in the CD spectra for the ligands will be purely result of the coiled coil. However, the intensity of the α-helical band will be compromised by the unusual positive CD signal of FIII9'-10 at 226 nm, representing aromatic contributions in the far-UV [29]. (CD scans for the ligands in the far and near UV regions in denaturing and non-denaturing buffer have been described previously [12].) To avoid contribution from FIII9'-10 aromatic residues in the far-UV, all experiments were performed in the presence of 6 M GdnHCl. Under these conditions both domains of FIII9'-10 are unfolded ($[GdnHCl]_{1/2}$ for FIII9' = 2 M, and for FIII10 = 4.5 M [10]), with the local environment of aromatic residues in the ligands being unordered [12], and therefore will not contribute to the CD signal at 222 nm.

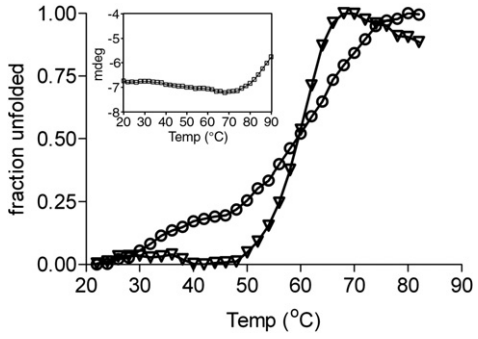

Fig. 5. Thermal unfolding of FIII9'-10-dimer (circles) and FIII9'-10-trimer (triangles) measured by circular dichroism at 222 nm. Proteins (1.0 mg/ml) were equilibrated in 6 M GdnHCl phosphate buffer in presence of 1 mM DTT. Insert shows raw data of thermal melt of FIII9'-10-tetramer.

The stability of the helical structure of the coiled coil domains of the ligands was therefore assessed by thermal unfolding profiles recorded by CD at 222 nm in 6 M GdnHCl (Fig. 5). For the reduced FIII9'-10-dimer and FIII9'-10-trimer the thermal unfolding profiles exhibited a sigmoid shape, indicating that unfolding of the helical structure was complete over the temperature range investigated. In contrast, the reduced FIII9'-10-tetramer appeared to be far more stable since no plateau was observed above 80 °C (the fraction unfolded therefore could not be calculated: raw CD data are shown in Fig. 5, insert). Interestingly, a two-step unfolding curve could be discerned for FIII9'-10-dimer: the first step between 25–45 °C and the second step approximating unfolding of FIII9'-10-trimer between 45–75 °C. While it would be tempting to speculate that this two-step unfolding curve represents unfolding of dimeric followed by trimeric FIII9'-10-dimer species, this would require further experimental corroboration. The T_m for FIII9'-10-trimer was 63 °C, with the T_m for FIII9'-10-dimer being similar (though not calculated due to the two-step curve) and the T_m of the FIII9'-10-tetramer being >80 °C. These values are comparable to the equivalent, isolated GCN4-derived peptides, albeit for thermal unfolding in 3 M GdnHCl [4], suggesting that fusion with FIII9'-10 does not destabilise the helical structure of the coiled coil.

Under non-reducing conditions, only small changes to the $CD_{222\ nm}$ signal were observed above 70 °C and no plateau was reached for any of the ligands (T_m>80 °C, data not shown). Therefore, disulphide formation between individual helices of the coiled coils confers stability during thermal unfolding, presumably since the helices are covalently linked at their C-termini. This is consistent with the similar increase in T_m observed for disulphide-bonded helices in the GCN4-derived coiled coils [27]. Compared to the FIII9'-10 domain pair, whose T_m determined by differential scanning calorimetry at pH 7 in non-denaturing buffer was 56 °C [23], the coiled coil is therefore an extremely stable oligomerisation partner. With respect to cell culture experiments performed at 37 °C the conformational stability and oligomerisation state of the ligands remains entirely intact.

In conclusion, this study fully characterises the oligomerisation state and stability of a series of novel oligomeric integrin α5β1 ligands in solution. This will be of importance to design of cell supports and biomaterials if we are to quantitatively relate the cell spreading response to integrin–ligand cluster size. In a wider context, we show that for fusion of GCN4-derived oligomerisation domains to protein domains, the tetrameric coiled coil is the most stable and well defined, with the predicted dimeric coiled coil being poorly defined and strongly dependent upon protein concentration.

Acknowledgements

This work was supported by the BBSRC, Grant Ref. BB/D522497/1, with instrument support from the EPSRC, Grant Ref. EP/E036244/1.

References

[1] J.J. Havranek, P.B. Harbury, Automated design of specificity in molecular recognition, Nat. Struct. Biol. 10 (2003) 45–52.
[2] A.N. Lupas, M. Gruber, The structure of alpha-helical coiled coils, Adv. Protein Chem. 70 (2005) 37–78.
[3] W.H. Landschulz, P.F. Johnson, S.L. McKnight, The leucine zipper: a hypothetical structure common to a new class of DNA binding proteins, Science 240 (1988) 1759–1764.
[4] P.B. Harbury, T. Zhang, P.S. Kim, T. Alber, A switch between two-, three-, and four-stranded coiled coils in GCN4 leucine zipper mutants, Science 262 (1993) 1401–1407.
[5] J. Willuda, S. Kubetzko, R. Waibel, P.A. Schubiger, U. Zangemeister-Wittke, A. Pluckthun, Tumor targeting of mono-, di-, and tetravalent anti-p185(HER-2) miniantibodies multimerized by self-associating peptides, J. Biol. Chem. 276 (2001) 14385–14392.
[6] L.Y. Koo, D.J. Irvine, A.M. Mayes, D.A. Lauffenburger, L.G. Griffith, Co-regulation of cell adhesion by nanoscale RGD organization and mechanical stimulus, J. Cell Sci. 115 (2002) 1423–1433.
[7] G. Maheshwari, G. Brown, D.A. Lauffenburger, A. Wells, L.G. Griffith, Cell adhesion and motility depend on nanoscale RGD clustering, J. Cell Sci. 113 (2000) 1677–1686.
[8] R.P. Grant, C. Spitzfaden, H. Altroff, I.D. Campbell, H.J. Mardon, Structural requirements for biological activity of the ninth and tenth FIII domains of human fibronectin, J. Biol. Chem. 272 (1997) 6159–6166.
[9] F. Coussen, D. Choquet, M.P. Sheetz, H.P. Erickson, Trimers of the fibronectin cell adhesion domain localize to actin filament bundles and undergo rearward translocation, J. Cell Sci. 115 (2002) 2581–2590.
[10] C.F. van der Walle, H. Altroff, H.J. Mardon, Novel mutant human fibronectin FIII9-10 domain pair with increased conformational stability and biological activity, Protein Eng. 15 (2002) 1021–1024.
[11] N. Watson, G. Duncan, W.S. Annan, C.F. van der Walle, A tetravalent RGD ligand for integrin-mediated cell adhesion, J. Pharm. Pharmacol. 58 (2006) 959–966.
[12] M. Kreiner, Z. Li, J. Beattie, S.M. Kelly, H.J. Mardon, C.F. van der Walle, Self-assembling multimeric integrin α5β1 ligands for cell attachment and spreading, Protein Eng. Des. Sel. 21 (2008) 553–560.
[13] P. Schuck, Size-distribution analysis of macromolecules by sedimentation velocity ultracentrifugation and Lamm equation modeling, Biophys. J. 78 (2000) 1606–1619.
[14] P. Schuck, On the analysis of protein self-association by sedimentation velocity analytical ultracentrifugation, Anal. Biochem. 320 (2003) 104–124.
[15] T.M. Laue, D.D. Shah, T.M. Ridgeway, S.L. Pelletier, in: S.E. Harding, A.J. Rowe, J.C. Horton (Eds.), Analytical Ultracentrifugation in Biochemistry and Polymer Science, Royal Society of Chemistry, Cambridge, UK, 1992, pp. 90–125.
[16] K. Arnold, L. Bordoli, J. Kopp, T. Schwede, The SWISS-MODEL workspace: a web-based environment for protein structure homology modeling, Bioinformatics 22 (2006) 195–201.
[17] L.J. Harris, S.B. Larson, K.W. Hasel, A. McPherson, Refined structure of an intact IgG2a monoclonal antibody, Biochemistry 36 (1997) 1581–1597.
[18] J. Garcia de la Torre, S. Navarro, M.C. Lopez Martinez, F.G. Diaz, J.J. Lopez Cascales, HYDRO: a computer program for the prediction of hydrodynamic properties of macromolecules, Biophys. J. 67 (1994) 530–531.
[19] O. Byron, Hydrodynamic bead modeling of biological macromolecules, Methods Enzymol. 321 (2000) 278–304.
[20] P.J. Fleming, N.C. Fitzkee, M. Mezei, R. Srinivasan, G.D. Rose, A novel method reveals that solvent water favors polyproline II over beta-strand conformation in peptides and unfolded proteins: conditional hydrophobic accessible surface area (CHASA), Protein Sci. 14 (2005) 111–118.
[21] W.S. Annan, M. Fairhead, P. Pereira, C.F. van der Walle, Emulsifying performance of modular beta-sandwich proteins: the hydrophobic moment and conformational stability, Protein Eng. Des. Sel. 19 (2006) 537–545.
[22] M. Amor-Mahjoub, J.P. Suppini, N. Gomez-Vrielyunck, M. Ladjimi, The effect of the hexahistidine-tag in the oligomerization of HSC70 constructs, J. Chromatogr., B 844 (2006) 328–334.
[23] P. Pereira, S.M. Kelly, A. Cooper, H.J. Mardon, P.R. Gellert, C.F. van der Walle, Solution formulation and lyophilisation of a recombinant fibronectin fragment, Eur. J. Pharm. Biopharm. 67 (2007) 309–319.
[24] P. Burkhard, S. Ivaninskii, A. Lustig, Improving coiled-coil stability by optimizing ionic interactions, J. Mol. Biol. 318 (2002) 901–910.
[25] P. Burkhard, M. Meier, A. Lustig, Design of a minimal protein oligomerization domain by a structural approach, Protein Sci. 9 (2000) 2294–2301.
[26] R.M. Thomas, A. Zampieri, K. Jumel, S.E. Harding, A trimeric, alpha-helical, coiled coil peptide: association stoichiometry and interaction strength by analytical ultracentrifugation, Eur. Biophys. J. 25 (1997) 405–410.
[27] E.K. O'Shea, R. Rutkowski, P.S. Kim, Evidence that the leucine zipper is a coiled coil, Science 243 (1989) 538–542.
[28] E.K. O'Shea, K.J. Lumb, P.S. Kim, Peptide 'Velcro': design of a heterodimeric coiled coil, Curr. Biol. 3 (1993) 658–667.
[29] M.Y. Khan, G. Villanueva, S.A. Newman, On the origin of the positive band in the far-ultraviolet circular dichroic spectrum of fibronectin, J. Biol. Chem. 264 (1989) 2139–2142.